Supplement of Atmos. Chem. Phys., 21, 5953–5964, 2021
https://doi.org/10.5194/acp-21-5953-2021-supplement

Supplement of

Firewood residential heating – local versus remote influence on the aerosol burden

Clara Betancourt et al.

Correspondence to: Iulia Gensch (i.gensch@fz-juelich.de)

S1 Selection of levoglucosan filter samples to be investigated

Table S1.1: Overview on selected LANUV filter samples from the STYR and EIFE sites. Sampling dates, filter levoglucsan loadings and main origin geographical regions for the investigated air parcels (determined by Hybrid Single-Particle Lagrangian Integrated Trajectory (HYSPLIT, http://ready.arl.noaa.gov/ HYSPLIT.php back trajectory analyses) are given. The sampling time is 24h and filters are daily changed at 00:00 UTC+1.

.	Sampling date (dd-mm-yy)	STYR LG / ng	STYR Main origin regions	EIFE LG / ng	EIFE Main origin regions
1	02-11-15	18910	Southeast Europe	9503	Southern Germany
2	06-11-15	10667	France / Atlantic Ocean	3976	France / Atlantic Ocean
3	10-11-15	15128	Atlantic Ocean	8437	Atlantic Ocean
4	14-11-15	3297	Atlantic Ocean (France, UK)	5140	Atlantic Ocean (France, UK)
5	22-11-15	65942	Arctic Ocean, Scandinavia	12219	Arctic Ocean, Scandinavia
6	26-11-15	12801	Arctic Ocean	3976	Arctic Ocean
7	08-12-15	20752	France, Mediterranean Sea	5915	France, Mediterranean Sea
8	10-02-16	65942	Southern / Eastern Europe	25019	Southern Europe
9	14-02-16	62936	Southern Germany, France	33262	Southern / Eastern Europe
10	18-02-16	8825	France, Atlantic Ocean, UK	3103	Southern Germany, France
11	26-02-16	89798	France	18619	Benelux, UK
12	05-03-16	30159	France, Benelux, UK	18716	France, Benelux, UK
13	09-03-16	26765	Southern Germany, France	15419	Southern Germany, France
14	13-03-16	68852	Eastern Europe	28026	Eastern Europe
15	17-03-16	13867	Eastern Europe	9213	Eastern Europe
16	19-01-17	235065	Eastern Europe	73778	Eastern Europe
17	27-01-17	37238	Southern Europe	10939	Southern Europe
18	12-02-17	60589	Southern Europe	28472	Southern Europe
19	20-03-17	25601	Atlantic Ocean	22886	Atlantic Ocean
20	24-03-17	16136	Europe	8922	Europe
21	28-03-17	23041	France, Southern Germany	10318	France, Southern Germany
22	01-04-17	14662	Benelux	6672	Benelux
23	13-04-17	12413	UK	5974	UK
24	17-04-17	26299	Northern Atlantic, UK	9542	Northern Atlantic, UK
25	21-04-17	4655	Northern Atlantic, UK	5818	Northern Atlantic, UK

Table S1.2: Average temperature during the sampling periods (from ECMWF meteorology)

	Sampling date [dd-mm-yy]	average temperature EIFE [°C]	average temperature STYR [°C]
1	02-11-15	8.81	7.77
2	06-11-15	14.14	14.98
3	10-11-15	11.88	13.70
4	14-11-15	7.04	8.13
5	22-11-15	0.89	2.07
6	26-11-15	2.42	3.71
7	08-12-15	9.63	10.31
8	10-02-16	2.47	4.02
9	14-02-16	1.64	2.14
10	18-02-16	0.66	1.74
11	26-02-16	0.91	1.65
12	05-03-16	0.88	2.66
13	09-03-16	2.18	3.82
14	13-03-16	2.49	3.45
15	17-03-16	3.29	5.31
16	19-01-17	-6.66	-1.84
17	27-01-17	0.44	1.50
18	12-02-17	2.28	2.62
19	20-03-17	9.25	10.80
20	24-03-17	7.81	8.77
21	28-03-17	13.23	12.82
22	01-04-17	11.19	12.72
23	13-04-17	8.53	9.49
24	17-04-17	4.94	6.54
25	21-04-17	7.46	9.15

S2 Experimental methods for measurement of levoglucosan concentration and isotopic composition

Concentration

Ambient levoglucosan concentrations were determined at LANUV by ion chromatography (871 Advanced Bioscan equipped with 818 IC Pump, Metrohm Deutschland GmbH, Filderstadt, Germany). The suspension was produced with 40 ml of ultrapure water in which up to six filter sections of 23 mm diameter are shaken for 60 min in a 50 ml PE centrifuge tube. Samples were injected intro chromatograph using a sample processor (Metrohm 853, Metrohm Deutschland GmbH, Filderstadt, Germany). Chromatography was conducted at 297 K with a flow of 0.7 ml min^{-1} at approx. 5.5 MPa using 1.5 g NaOH and 0.4 g sodium acetate in 1 kg of water as an eluent. More details concerning the method applied for determination of levoglucosan concentrations can be found in (Pfeffer et al., 2013). The detection limit of this method was determined to be at 10 ng m-3.

Isotopic composition

LiquidExtraction ThermoDesorption TwoDimensionalGasChromatography IsotopeRatioMassSpectrometry (LE-TD-2DGC-IRMS) is employed off-line to determine levoglucosan isotope ratios in the sampled aerosol particles. The method developed by (Gensch et al., 2018) was further optimized, to improve the precision and accuracy of the heart-cut TD-2DGC-IRMS measurements. To avoid matrix effects, which lead to a lack of the GC separation efficiency, a HPLC-purification of the samples was integrated in the methodology. Small filter cuts are extracted twice by 10 ml Milli-Q water each in an ultrasonic bath (BANDELIN electronic GmbH, Berlin, Germany) for 15 min. The extracts are filtered using membrane filter Millex GP 13mm PES 0.22µm (Merk KGaA, Darmstadt, Germany). The two fractions of extracts and the portion used to rinse the vial walls were mixed together and directly transferred into a TurboVap 500 Evaporator Workstation (John Morris Scientific, Sydney, Australia). This was beforehand cleaned with Millipore water and ethanol (99.99 %, Merk KGaA, Darmstadt, Germany). The collected solution was concentrated at 333K to a volume of ca. 0.5 ml. This batch is transferred to a 1.5 ml vial. The walls of the TurboVap vessels were rinsed three times with a total of 0.4 ml Milli-Q water, which are added to the concentrate, which is then placed in a freezer kept at 257K. The frozen samples are freeze-dried using a freeze-dryer Christ Alpha 1-2 LD plus (Martin Christ Gefriertrocknungsanlagen GmbH, Germany). The pressure is immediately reduced to 2-3Pa. In that way the samples stay solid. Under 611Pa, the sublimation starts. Since the instrument is not thermo-isolated, the samples slowly took the temperature of the surroundings, intensifying the ongoing sublimation process. 100 µl Milli-Q water are added to the dried samples. To reduce matrix effects, the aqueous sample extracts are 'purified' by high performance liquid chromatography (HPLC) using a polar Carbohydrate Ca2+ column (10x4 mm CS-Chromatographie, Langerwehe) and water as eluent. At the front of the separating column, a pre-column (MultoHigh 100RP 18-3 µm, 10x4 mm length) (Carbohydrate Ca^ (2+) 10*4mm Chromatographie Service GmbH, Langerwehe, Germany) is attached, to avoid contaminations of the main column. For the levoglucosan detection, a differential refractometer (KNAUER GmbH, Berlin, Germany), is used. The solvent reservoir is filled with Millipore water. The column was flushed with this eluent for half an hour, to clean the system and to stabilize the base line. The flow rate through the capillary tube is 0.75 ml min^{-1}. The pressure is kept at 64 bar. The column oven temperature is set to 298 K . The analyte extracts are injected in the HPLC and the fraction containing levoglucosan are collected into glass vials. During the HPLC sampling window, ca 1.5 mL levoglucosan eluent is collected. To prevent the presence of water in the CG-IRMS system, water must be removed by freeze-drying. After the freeze drying of the HPLC solutions, the vial walls are thoroughly rinsed using methanol. A rigorous wash-out, by repeated rinsing-concentrating procedures, is mandatory to prevent any wall losses which can lead at this trace amount level of investigated compound even to a complete waste of levoglucosan. Eventually, the volume of dissolving methanol adjusted to reach a concentration of ~200 ng/µl . The vials are stored in a refrigerator at 277 K until the isotopic measurements.

The instrumental setup for isotopic measurements consists of three major sections (i) a thermal desorption/cryo focusing unit , (ii) a gas-chromatograph-separation unit and (iii) a Detection unit. The aim of the first unit is to concentrate and focus the compounds prior to injection into the gas chromatograph. This section consists of two components; a Thermal Desorption Unit (TDU) (GERSTEL GmbH, Germany) mounted on the top of a Cooled Injection System (CIS) (GERSTEL GmbH, Germany). The TDU utilizes heat and flow of inert gas (He, 99.9999 % AIR LIQUID GmbH, Germany) to thermo-desorb the analyte mixture from the quartz wool placed in a TDU tube. The compounds are volatilized and then trapped in the CIS at low temperature. The CIS is subsequently heated to release the organic compounds and transfer them into the GC (Agilent 6890, Agilent Technologies USA). Two dimensional GC is used to separate the component of interest from the others in the mixture. It is equipped with two columns. The first column is nonpolar (Rtx-1301, 30 m length, 0.32 mm i.d., 0.25 µm film thickness), being used to separate the compounds depending on their volatility. The second column (FS-OV-225-CB -0.25, 30 m length, 0.25 mm i.d., 0.25 µm film thicknesses) is polar and utilized for a better resolution and selectivity of polar compounds and thus, to optimally separate the levoglucosan. Two four port valves are mounted on the GC to choose different operating configurations and thus to enable the two dimensional 'heart-cut' separation. According to that, during the heart-cut stage, the eluent is directed through the first column into the additional Cryo Trapped System (CTS) , were the compounds of interest are trapped at very low temperatures . After separation by the second column, 25% of the sample is sent to the Mass Spectrometer Detector (MSD) (5975C inert XL MSD, Agilent technologies, USA), whereas the rest of the sample is transferred to the oxidation reactor (Thermo Scientific Bremen, Germany), where the hydrocarbons are completely oxidized to CO2 and water. The water is removed by using a semi permeable Nafion membrane (Thermo Scientific GmbH., Bremen, Germany). The carbon dioxide is transferred to the Isotope Ratio Mass Spectrometer (IRMS) via a continuous flow, open split device (ConFlo-IV) (Thermo Scientific GmbH., Bremen, Germany).

The Heart Cut TD-2DGC-IRMS Method: 1 μL of the pre-cleaned mixture is injected on a small piece of quartz wool placed inside a the TDU glass tube (60 mm, 4 mm i.d., preconditioned at 623 K for 4 hours with 100 ml min^{-1} He flow). The tube is introduced into the TDU. The thermal desorption of the analytes spread on the wool is obtained by ramping the temperature of the TDU from 318 to 573 K at a rate of 500 K min−1. The thermo-desorbed mixture is thus sent to the CIS (set at 243 K) by helium at a vent flow of 150 ml min−1. After complete trapping, the CIS is heated to 503 K at a rate of 12K s^{-1}. The focused compound mixture is transferred splitless at 2.5 ml min^{-1} to the GC. The GC oven temperature program depends of the used dimension of the GC separation. For the preliminary run to determine the levoglucosan retention time (RT), only one temperature-increasing ramp is run. The initial temperature is kept for 10 min at 333 K. Subsequently, the temperature is ramped to 473 K at a rate of 10 K min−1 maintaining it for 10 min. The derived RT for levoglucosan is 14.3 min. The two dimensional separation is achieved in three stages: (i) from 0-11.5 min, the eluent from column 1 is directed to the FID; (ii) after 11.5 min, the four-port valves are switched to trigger the transfer of the column 1 eluent to the CTS, which was previously cooled to 173 K. (iii) At 19.5 minutes, both valves are switched to establish the configuration for separation on column 2. At 20 min, the CTS is abruptly heated (at 20K s^{-1} to 473 K, to send the thermo-desorbed compounds into the second column. The separated compounds are sent to MSD for the peak identification and to IRMS for the isotope ratios measurements. When using the heart-cut two-dimensional GC separation, two ramps in the oven temperature program are necessary. The initial temperature is 353K, being maintained for 1 min. During the 'transfer' and 'trapping' stages, the oven temperature was increased by 10 K min^{-1} to 473 K and was kept there for 1 min , till the end of the heart-cut time window (from 11.5 to 19.5 min). At 16 min, the oven is cooled to 363 K at a rate of 50K min^{-1} and kept for 1 min. The temperature is then ramped to 513 K at a rate of 5 K min−1 and maintained there for 10 min for the separation on the second column. The heart-cut 2DGC method delivers base-line, well separated peaks.

S3 Basic statistics of measurement results

Table S3: Basic statistics of the experimental results. For the frequency distribution analysis, the concentration and isotope ratio data were divided in 25 ng m-3 and 0.5 ‰ bins, respectively. For the observed number of occurrences, Gauss functions were fitted. The amplitudes, mean values and 1σ standard deviations are given for the derived modes.

	EIFE	**STYR**
Number of samples	25	25

Concentration / ng m^{-3}

	EIFE	STYR
mean	54.18	152.13
std deviation	35.80	124.09

	EIFE	STYR
min	12.36	25.41
10% percentile	18.46	41.72
median	30.19	85.26
90% percentile	104.21	282.10
max	156.74	509.48

	EIFE	STYR
Frequency distribution	amplitude: 9.9 ± 1.0 mean: 34.8 ± 2.4 σ: 19.5 ± 2.2	amplitude: 5.3 ± 0.6 mean: 62.4 ± 3.4 σ: 28.0 ± 3.5 amplitude: 2.9 ± 0.4 mean: 204.5 ± 4.3 σ: 24.6 ± 4.3

δ^{13}C / ‰

	EIFE	STYR
mean	-23.50	-23.43
std	0.99	1.03

	EIFE	STYR
min	-25.78	-26.26
10% percentile	-24.53	-24.63
median	-23.55	-23.30
90% percentile	-22.64	-22.21
max	-21.30	-21.79

	EIFE	STYR
Frequency distribution	amplitude: 6.4 ± 1.0 mean: -23.3 ± 0.1 σ: 0.7 ± 0.1	amplitude: 5.4 ± 0.4 mean: -23.3 ± 0.1 σ: 0.9 ± 0.1

S4 Modeling method

The modeling setup (Figure S4) provides a framework for the source apportionment of biomass burning aerosol and its fate during transport. Gridded meteorological input data delivers the necessary wind fields to describe transport by advection and diffusion. FLEXPART is run backwards from the sampling points to investigate the origin of the sampled air masses. Chemical loss and deposition are included in the runs. The output of a backwards run is called ‚retroplume‘, and represents sensitivity fields of the receptor to potential upwind sources. Retroplumes can be linked with emission inventories, using the ‚folded retroplume technique‘. For this, a footprint layer that contains the emissions is defined. Since the case study is carried out in the cold season, levoglucosan emissions originate mainly from domestic heating with firewood. The result of the folding is a data field that describes the contribution of individual upwind domestic heating sources to the receptor. Adding up all contributions, the concentration at the receptor is obtained. When releasing two isotope tracers ^{12}LG and ^{13}LG δ^{13}C can be calculated at the receptor. These modeling results can be compared with isotopic- and concentration measurements at the sampling sites. A closure study between modeling and measurements validates the modeling and leads to a better understanding of sources and processes of biomass burning aerosol.

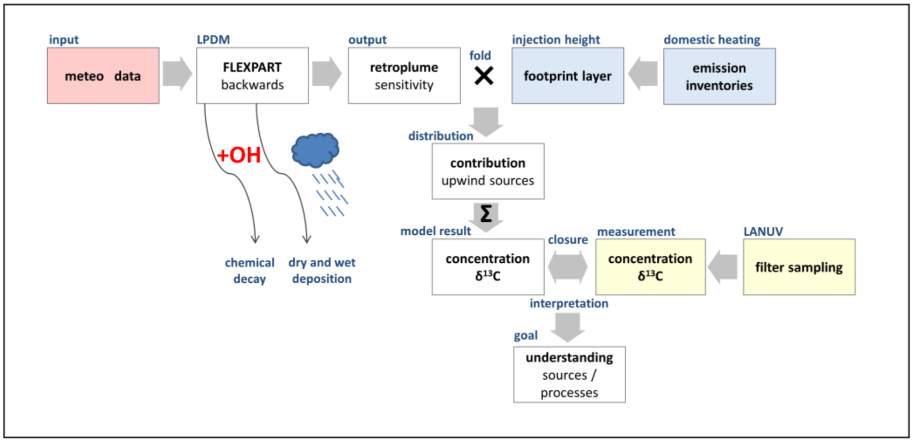

Figure S4: Modeling flow chart. Details are given in the text.

S5 Approach to determine levoglucosan emission inventories for firewood burning in the cold season, used to initialize the FLEXPART concentration and isotopic calculations

In the following, we derive from known data levoglucosan emission fields, $S = \frac{m_{LG}}{A \cdot t}$, which are required for the folding calculations to determine levoglucosan concentration and isotopic composition at the receptor.
To this end, the annual firewood consumption of European countries, provided by the United Nations[1], is divided by the total population of each country to obtain the per capita and time consumption of firewood$\left(\frac{V_{firewood}}{N_{person} \cdot t}\right)$. There are several studies that divide living areas into the different categories ‚city‘, ‚suburbs‘, ‚close to a city‘ and ‚rural‘ (Döring et al., 2016), or address wood stove exhaust down to the single chimney (Baumbach et al., 2010). Such consideration is beyond the scope of this Europe-wide study. Here, the per capita consumption is weighted with the population density $\left(\frac{N_{person}}{A}\right)$ which is given with a spatial resolution of 0.25° × 0.25°, yielding a continuous area consumption of firewood with the same resolution$\left(\frac{V_{firewood}}{A \cdot t}\right)$.
Levoglucosan emission fields are derived as following:

$$S = f_v \cdot f_{LG} \cdot \frac{V_{firewood}}{A \cdot t}$$

where f_v is a density conversion factor of 500±200 kg m^{-3} (Döring et al., 2016) and f_{LG} is the average emission factor of 200 mg LG kg^{-1} for firewood. Furthermore the consumption is weighted with individual factors[2] for every month, to describe seasonal variability in the wood consumption. Uncertainties are related to density variability of woods used in Europe for heating, different heating behaviour as well as unresolved f_{LG} due to e.g. unknown type of firewood or burning conditions, (Akagi et al., 2011) and references therein.
The domestic heating emission enters the atmosphere as a hot plume of wood smoke with an injection height of 100-300 m (Hueser et al., 2017). This ‘footprint layer’ contains the volume emission data needed for the folding calculations: $\frac{m_{LG}}{V \cdot t}$
To this end, the retroplume transmission corrected residence time (Seibert and Frank, 2004) in the grid cell is multiplied with the emission being injected into that cell to determine the contribution of individual sources to the levoglucosan concentration at the receptor $\left(\frac{m_{LG}}{V}\right)$.

---

[1] Firewood combustion data is obtained from statistical databases provided by the United Nations: data.un.org/Data.aspx?d=EDATA&f=cmID%3aFW%3btrID%3a1231, access March 10th 2017.
[2] Monthly weighting is estimated from a personal survey.

Adding up all contributions from all sources, the concentration at the receptor is determined:

$$C = \sum \frac{m_{LG}}{V}$$

Furthermore, for isotope ratio calculation it must be considered that the ^{13}LG emissions can be derived from the source isotopic ratio:

$$S_{^{13}LG} = \frac{m_{^{13}LG}}{A \cdot t} = \frac{m_{^{12}LG} \cdot R_0}{A \cdot t} = R_0 \cdot S_{^{12}LG}$$

where $S_{^{12}LG}$ and $S_{^{13}LG}$ are the emissions of the two levoglucosan isotopologues and R_0 is the source specific isotope ratio. T The residence times $t_{res,^{12}LG}$ and $t_{res,^{13}LG}$ are calculated in the retroplumes depending on the rate for the photo-chemical degradation of ^{12}LG and ^{13}LG by OH, respectively. Thus, the absolute isotope ratios R_t can be obtained in each grid and thus, at the receptor.

$$R_t = \frac{\sum \frac{m_{^{13}LG}}{V \cdot t} \cdot t_{res,^{13}LG}}{\sum \frac{m_{^{12}LG}}{V \cdot t} \cdot t_{res,^{12}LG}}$$

S6 Model results using ECMWF vs. GFS meteorological input data

Table S6.1: Comparison of model results obtained with ECMWF/GFS meteorological input data at the EIFE station. Differences for the $\delta^{13}C$ and concentration data are given in ‰ and %, respectively.

	EIFE	ECMWF	GFS		ECMWF	GFS	
Nr.	Sampling date (dd-mm-yy)	δ_{mod} / ‰	δ_{mod} / ‰	δ_{diff} / ‰	c_{mod} / ng m^{-3}	c_{mod} / ng m^{-3}	c_{diff} / %
1	02-11-15	-23.02	-23.11	-0.09	59.79	55.84	-6.61
2	06-11-15	-23.48	-23.48	0.00	23.96	25.38	5.93
3	10-11-15	-23.35	-23.43	-0.08	44.45	33.82	-23.91
4	14-11-15	-23.49	-23.47	0.02	28.93	31.42	8.59
5	22-11-15	-23.63	-23.71	-0.07	19.78	18.05	-8.76
6	26-11-15	-23.68	-23.71	-0.03	19.48	18.50	-5.01
7	08-12-15	-23.11	-23.18	-0.07	47.03	40.40	-14.08
8	10-02-16	-23.53	-23.53	-0.01	26.37	25.89	-1.84
9	14-02-16	-23.05	-23.01	0.04	79.93	83.21	4.10
10	18-02-16	-22.88	-22.88	0.00	50.91	51.66	1.46
11	26-02-16	-23.32	-23.37	-0.05	36.90	32.32	-12.42
12	05-03-16	-23.30	-23.17	0.13	39.11	72.83	86.22
13	09-03-16	-23.06	-23.10	-0.04	52.10	50.75	-2.58
14	13-03-16	-23.22	-23.26	-0.03	36.08	32.21	-10.73
15	17-03-16	-23.01	-22.99	0.02	60.03	60.66	1.05
16	19-01-17	-23.27	-23.42	-0.15	38.93	26.46	-32.04
17	27-01-17	-22.98	-23.09	-0.11	65.05	45.85	-29.51
18	12-02-17	-22.87	-22.98	-0.11	98.36	62.45	-36.50
19	20-03-17	-23.46	-23.52	-0.06	31.37	26.64	-15.07
20	24-03-17	-22.97	-23.13	-0.15	61.40	42.05	-31.52
21	28-03-17	-23.17	-23.17	0.00	51.47	46.08	-10.46
22	01-04-17	-23.53	-23.43	0.10	20.72	27.06	30.62
23	13-04-17	-23.67	-23.74	-0.07	19.48	17.34	-11.01
24	17-04-17	-23.66	-23.69	-0.02	19.68	19.07	-3.12
25	21-04-17	-23.46	-23.57	-0.11	24.98	21.02	-15.85

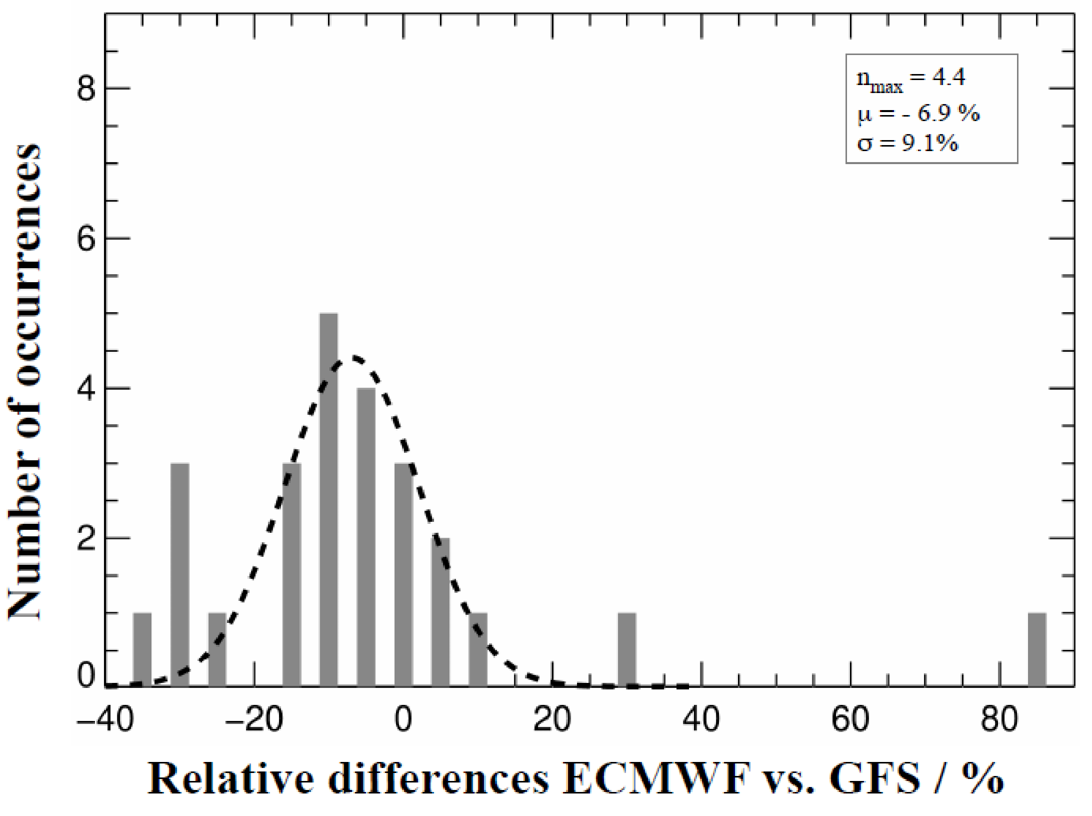

195 **Figure S6.1:** Distribution frequency of the relative differences in the calculated concentrations by using ECMWF vs. GFS meteorological data at the EIFE site

Table S6.2: Comparison of model results obtained with ECMWF/GFS meteorological input data at the STYR station. Differences for the $\delta^{13}C$ and concentration data are given in ‰ and %, respectively.

STYR

Nr.	Sampling date (dd-mm-yy)	ECMWF δ mod / ‰	GFS δ mod / ‰	δ diff / ‰	ECMWF c mod / ng m^{-3}	GFS c mod / ng m^{-3}	c diff / %
1	02-11-15	-23.09	-23.16	-0.07	81.17	75.02	-7.58
2	06-11-15	-23.32	-23.32	0.00	42.43	44.14	4.02
3	10-11-15	-23.51	-23.53	-0.01	28.66	27.90	-2.66
4	14-11-15	-23.56	-23.57	-0.02	25.89	24.88	-3.89
5	22-11-15	-23.63	-23.66	-0.03	21.02	20.01	-4.80
6	26-11-15	-23.60	-23.62	-0.02	24.26	23.19	-4.40
7	08-12-15	-23.15	-23.20	-0.05	56.56	45.69	-19.22
8	10-02-16	-23.49	-23.51	-0.03	29.84	28.28	-5.25
9	14-02-16	-23.06	-23.07	-0.01	152.61	151.53	-0.71
10	18-02-16	-22.91	-22.91	0.00	75.21	82.50	9.70
11	26-02-16	-23.32	-23.29	0.03	55.14	62.79	13.87
12	05-03-16	-23.18	-23.30	-0.12	108.46	70.36	-35.13
13	09-03-16	-23.01	-23.06	-0.05	64.39	65.64	1.94
14	13-03-16	-23.26	-23.29	-0.03	44.16	38.95	-11.81
15	17-03-16	-23.17	-23.16	0.00	67.41	64.24	-4.70
16	19-01-17	-23.33	-23.39	-0.05	51.36	46.94	-8.60
17	27-01-17	-23.00	-23.09	-0.09	91.16	72.01	-21.01
18	12-02-17	-22.88	-22.95	-0.08	112.18	106.81	-4.79
19	20-03-17	-23.46	-23.40	0.06	33.47	40.58	21.25
20	24-03-17	-23.13	-23.25	-0.12	57.77	47.79	-17.28
21	28-03-17	-23.06	-23.04	0.02	76.51	83.52	9.16
22	01-04-17	-23.35	-23.29	0.06	36.94	47.42	28.37
23	13-04-17	-23.77	-23.77	0.00	16.99	16.90	-0.56
24	17-04-17	-23.64	-23.63	0.01	21.74	21.95	0.95
25	21-04-17	-23.60	-23.66	-0.06	21.23	19.75	-7.00

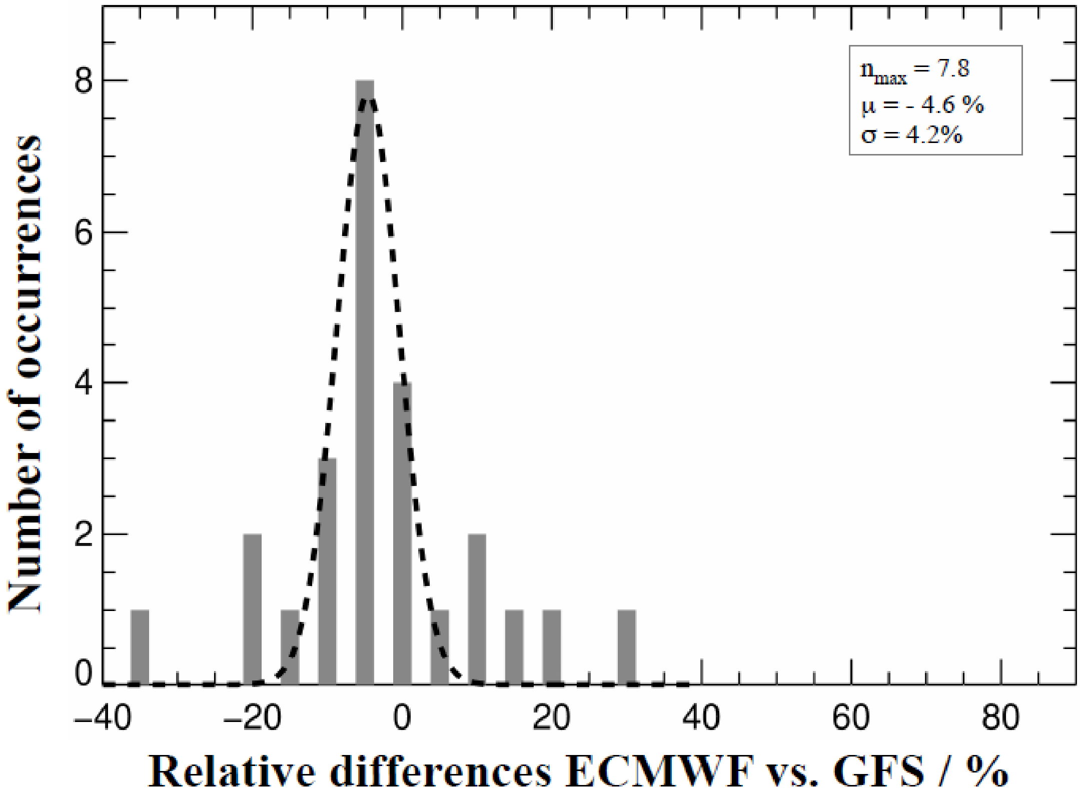

Figure S6.2: Distribution frequency of the relative differences in the calculated concentrations by using ECMWF vs. GFS meteorological data at the STYR site

S7 Modeled and observed aerosol age

Table S7.1: Percentage concentration contribution of each day before sampling to the filter loadings. Discrete categories 'one –', 'two-', 'three days old particles', as well as 'particle older than three days' are given as fractions of the concentration contributions.

		EIFE				STYR			
Nr.	Sampling date (dd-mm-yy)	day 1 %	day 2 / %	day 3 / %	day 4-7 / %	day 1 / %	day 2 / %	day 3 / %	day 4-7 / %
1	02-11-15	11.20	37.40	34.80	16.60	38.00	33.30	19.00	9.70
2	06-11-15	35.60	36.10	19.80	8.50	66.70	19.30	10.20	3.84
3	10-11-15	67.50	32.50	0.00	0.00	80.60	19.40	0.00	0.00
4	14-11-15	80.80	19.20	0.00	0.00	92.10	7.89	0.00	0.00
5	22-11-15	52.60	32.10	11.40	3.99	78.50	14.70	4.76	1.99
6	26-11-15	80.60	19.40	0.00	0.00	95.40	4.64	0.00	0.00
7	08-12-15	19.90	42.60	16.40	21.00	40.10	33.50	13.70	12.70
8	10-02-16	63.50	34.00	0.17	2.37	72.60	23.80	0.37	3.26
9	14-02-16	16.20	57.00	19.80	6.96	42.20	40.60	12.10	5.05
10	18-02-16	6.40	18.00	30.30	45.40	26.70	19.60	22.30	31.40
11	26-02-16	31.40	57.90	10.30	0.44	81.70	17.00	1.29	0.00
12	05-03-16	22.10	76.70	1.20	0.00	59.70	38.60	1.74	0.00
13	09-03-16	26.60	35.90	15.10	22.40	34.60	28.30	11.90	25.90
14	13-03-16	29.70	36.80	10.60	22.80	63.20	20.30	2.14	14.40
15	17-03-16	18.40	30.80	23.00	27.80	55.30	24.20	8.82	11.70
16	19-01-17	45.10	33.60	7.96	13.40	76.90	17.90	3.27	1.95
17	27-01-17	19.80	36.10	16.80	27.40	32.20	31.80	16.40	19.50
18	12-02-17	14.20	37.50	16.80	31.50	19.20	30.40	19.90	30.50
19	20-03-17	63.00	37.00	0.00	0.00	83.80	16.20	0.00	0.00
20	24-03-17	16.30	21.10	25.60	37.00	41.70	20.80	13.60	23.80
21	28-03-17	41.90	23.80	22.30	11.90	33.60	27.30	22.90	16.20
22	01-04-17	34.50	34.50	11.10	19.90	50.60	41.00	4.06	4.30
23	13-04-17	69.20	30.70	0.09	0.00	89.10	10.90	0.02	0.00
24	17-04-17	57.80	41.60	0.33	0.24	82.60	16.90	0.11	0.37
25	21-04-17	27.50	47.50	16.90	8.01	56.70	28.80	6.78	7.69

Table S7.2: Basic statistics for $\boldsymbol{t_{av,traj}}$

Site	Average	Standard deviation	N	Error of mean
EIFE	1.6 d	0.6 d	25	0.1 d
STYR	1.1 d	0.5 d	25	0.2 d
All	1.3 d	0.6 d	50	0.1 d

Table S7.3: Basic statistics for $\boldsymbol{t_{av,obs}}$

Site	Average	Standard deviation	N	Error of mean
EIFE	-1.1 d	3.8 d	25	0.8 d
STYR	-0.3 d	3.3 d	25	0.7 d
All	-0.7 d	3.6 d	50	0.5 d

Table S7.4: Basic statistics for the difference between $\boldsymbol{t_{av,traj}}$ and $\boldsymbol{t_{av,obs}}$

Site	Average	N	Error of mean	Estimated $\delta^{13}C_0$ / ‰
EIFE	2.7 d	25	0.8 d	-24.0
STYR	1.4 d	25	0.7 d	-23.9
All	2.0 d	50	0.5 d	-23.7

S8 Modeled loss processes

Table S8.1: Model tracer specifications which are relevant for loss processes. Here the density (ρ), the diameter (D) of the particles, as well as the OH reaction constant (k_{OH}) and the coalescence probability (P_{coal}) are given.

SPECIES	ρ / g cm^{-3}	D / µm	k_{OH} / cm^3 molec^{-1} s^{-1}	P_{coal}
"inert"	-	-	-	-
"chem"	-	-	2.67×10^{-12}	-
"drydep"	1.4	0,25±1,5	2.67×10^{-12}	-
"wetdep"	1.4	0,25±1,5	2.67×10^{-12}	1

Table S8.2: Model results obtained for the EIFE station when implementing different loss processes**.**

EIFE

Nr.	date (dd-mm-yy)	c inert / ng m^{-3}	δ inert / ‰	c chem / ng m^{-3}	δ chem / ‰	c drydep / ng m^{-3}	δ drydep / ‰	c wetdep / ng m^{-3}	δ wetdep / ‰
1	02-11-15	72.77	-23.37	61.12	-23.01	59.79	-23.02	59.79	-23.02
2	06-11-15	26.04	-23.61	24.33	-23.47	23.98	-23.48	23.96	-23.48
3	10-11-15	46.50	-23.42	44.99	-23.35	44.45	-23.35	44.45	-23.35
4	14-11-15	29.89	-23.54	29.18	-23.49	28.93	-23.49	28.93	-23.49
5	22-11-15	20.59	-23.70	19.90	-23.63	19.79	-23.63	19.78	-23.63
6	26-11-15	19.80	-23.71	19.54	-23.68	19.48	-23.68	19.48	-23.68
7	08-12-15	56.48	-23.41	48.25	-23.10	47.07	-23.11	47.03	-23.11
8	10-02-16	27.21	-23.57	26.56	-23.52	26.39	-23.53	26.37	-23.53
9	14-02-16	94.07	-23.33	82.29	-23.05	80.15	-23.05	79.93	-23.05
10	18-02-16	68.62	-23.40	52.52	-22.86	51.00	-22.88	50.91	-22.88
11	26-02-16	39.89	-23.47	37.08	-23.31	36.90	-23.32	36.90	-23.32
12	05-03-16	42.52	-23.45	39.54	-23.30	39.20	-23.30	39.11	-23.30
13	09-03-16	63.00	-23.39	53.01	-23.05	52.15	-23.06	52.10	-23.06
14	13-03-16	42.11	-23.47	36.73	-23.21	36.10	-23.22	36.08	-23.22
15	17-03-16	73.41	-23.37	61.36	-23.00	60.08	-23.01	60.03	-23.01
16	19-01-17	43.86	-23.45	39.74	-23.26	38.99	-23.27	38.93	-23.27
17	27-01-17	81.76	-23.35	67.26	-22.96	65.06	-22.98	65.05	-22.98
18	12-02-17	127.70	-23.30	102.17	-22.86	98.61	-22.87	98.36	-22.87
19	20-03-17	32.47	-23.52	31.61	-23.46	31.37	-23.46	31.37	-23.46
20	24-03-17	76.42	-23.36	62.89	-22.96	61.47	-22.97	61.40	-22.97
21	28-03-17	58.49	-23.39	52.15	-23.16	51.47	-23.17	51.47	-23.17
22	01-04-17	22.59	-23.68	20.86	-23.52	20.72	-23.53	20.72	-23.53
23	13-04-17	19.86	-23.71	19.55	-23.67	19.48	-23.67	19.48	-23.67
24	17-04-17	20.11	-23.70	19.76	-23.66	19.69	-23.66	19.68	-23.66
25	21-04-17	26.88	-23.60	25.12	-23.46	24.98	-23.46	24.98	-23.46
			Mean of differences	-2.79	+0.21	-0.81	-0.01	-0.04	-0.00
				chem to inert		*drydepo to chem*		*wetdep to drydep*	

Table S8.3: Comparison between the scenarios using a background levoglucosan of 12.4 ng m^{-3} vs no background

	Background			No background		
Site	Slope	Std. Dev.	R^2	Slope	Std. Dev.	R^2
EIFE	1.35	0.24	0.58	1.73	0.15	0.85
STYR	1.93	0.66	0.27	2.98	0.44	0.66
All	2.08	0.43	0.33	2.61	0.28	0.64

Table S8.4: Model results obtained with different loss processes for the STYR station**.**

STYR

Nr.	date (dd-mm-yy)	c inert / ng m^{-3}	δ inert / ‰	c chem / ng m^{-3}	δ chem / ‰	c drydep / ng m^{-3}	δ drydep / ‰	c wetdep / ng m^{-3}	δ wetdep / ‰
1	02-11-15	93.33	-23.32	82.79	-23.08	81.19	-23.09	81.17	-23.09
2	06-11-15	45.68	-23.43	43.11	-23.31	42.48	-23.32	42.43	-23.32
3	10-11-15	29.28	-23.54	28.84	-23.51	28.66	-23.51	28.66	-23.51
4	14-11-15	26.33	-23.58	26.01	-23.55	25.90	-23.56	25.89	-23.56
5	22-11-15	21.51	-23.67	21.09	-23.63	21.02	-23.63	21.02	-23.63
6	26-11-15	24.42	-23.61	24.29	-23.59	24.26	-23.60	24.26	-23.60
7	08-12-15	65.31	-23.38	57.83	-23.14	56.61	-23.15	56.56	-23.15
8	10-02-16	30.76	-23.53	30.01	-23.48	29.85	-23.49	29.84	-23.49
9	14-02-16	174.18	-23.27	156.79	-23.05	153.04	-23.06	152.61	-23.06
10	18-02-16	96.34	-23.33	77.17	-22.90	75.31	-22.91	75.21	-22.91
11	26-02-16	56.92	-23.38	55.34	-23.32	55.15	-23.32	55.14	-23.32
12	05-03-16	115.15	-23.29	109.19	-23.18	108.63	-23.18	108.46	-23.18
13	09-03-16	78.79	-23.36	65.50	-23.00	64.46	-23.01	64.39	-23.01
14	13-03-16	49.10	-23.42	44.55	-23.25	44.17	-23.26	44.16	-23.26
15	17-03-16	74.97	-23.35	68.17	-23.16	67.43	-23.17	67.41	-23.17
16	19-01-17	53.35	-23.39	51.71	-23.33	51.39	-23.33	51.36	-23.33
17	27-01-17	111.20	-23.31	94.15	-22.98	91.20	-23.00	91.16	-23.00
18	12-02-17	143.88	-23.29	116.08	-22.86	112.43	-22.88	112.18	-22.88
19	20-03-17	34.24	-23.50	33.67	-23.46	33.48	-23.46	33.47	-23.46
20	24-03-17	66.45	-23.37	58.66	-23.12	57.81	-23.13	57.77	-23.13
21	28-03-17	88.98	-23.33	77.59	-23.05	76.52	-23.06	76.51	-23.06
22	01-04-17	39.40	-23.47	37.22	-23.35	36.95	-23.35	36.94	-23.35
23	13-04-17	17.08	-23.78	17.01	-23.77	16.99	-23.77	16.99	-23.77
24	17-04-17	21.96	-23.65	21.77	-23.64	21.75	-23.64	21.74	-23.64
25	21-04-17	22.07	-23.66	21.32	-23.60	21.23	-23.60	21.23	-23.60
			Mean of differences	-6.43	+0.16	-0.88	-0.01	-0.05	-0.00
				chem to inert		*drydepo to chem*		*wetdep to drydep*	

S9 Details of modeling and measurements results

An overview of the modeling and measurements results are given in the end of this supporting information (Pages 23-28)

References

Akagi, S. K., Yokelson, R. J., Wiedinmyer, C., Alvarado, M. J., Reid, J. S., Karl, T., Crounse, J. D., and Wennberg, P. O.: Emission factors for open and domestic biomass burning for use in atmospheric models, Atmos. Chem. Phys., 11, 4039-4072, 10.5194/acp-11-4039-2011, 2011.

Baumbach, G., Struschka, M., Juschka, W., Carrasco, M., Ang, K. B., Hu, L., Bächlin, D. W., and Sörgel, C.: Modellrechnungen zu den Immissionsbelastungen bei einer verstärkten Verfeuerung von Biomasse in Feuerungsanlagen der 1. BImSchV, Umweltbundesamt, 297, 2010.

Döring, P., Glasenapp, S., and Mantau, U.: Rohstoffmonitoring Holz. Energieholzverwendung in privaten Haushalten 2014. Marktvolumen und verwendete Holzsortimente., Universität Hamburg, 2016.

Gensch, I., Sang-Arlt, X. F., Laumer, W., Chan, C. Y., Engling, G., Rudolph, J., and Kiendler-Scharr, A.: Using δ13C of Levoglucosan As a Chemical Clock, Environ. Sci. Technol., 52, 11094-11101, 10.1021/acs.est.8b03054, 2018.

Hueser, I., Harder, H., Heil, A., and Kaiser, J. W.: Assumptions about footprint layer heights influence the quantification of emission sources: a case study for Cyprus, Atmos. Chem. Phys., 17, 10955-10967, 10.5194/acp-17-10955-2017, 2017.

Pfeffer, U., Breuer, L., Gladtke, D., and Schuck, T. J.: Contribution of wood burning to the exceedance of PM10 limit values in north rhine-westphalia, Gefahrstoffe - Reinhalt. Luft, 73, 239-245, 2013.

Seibert, P., and Frank, A.: Source-receptor matrix calculation with a Lagrangian particle dispersion model in backward mode, Atmos. Chem. Phys., 4, 51-63, 10.5194/acp-4-51-2004, 2004.

Overview EIFE 1/3

δ emis (t=0) = -23.2029 ‰
δ backgr = -23.9931 ‰
c backgr = 12.4 ng/m^3

Number	Date	δ exp [‰]	c exp [ng/m^3]	δ mod [‰]	c mod [ng/m^3]	backgr mod [%]	emis mod [%]	Plume (footprint layer, background)	Folded plume (incl. background)	emis mod day1 / 2 / 3 / r [%]	Emission contribution(d1, d2, d3, r)	Info
1	02-11-15	-23.70 ± 0.18	44.66 ± 4.91	-23.02	59.79	20.74	79.26	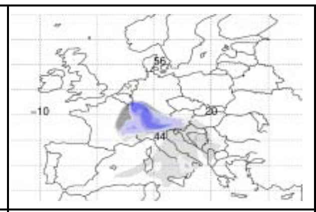	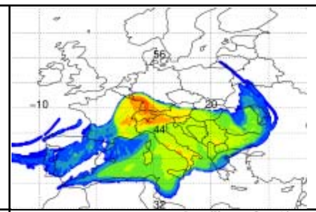	11,2 / 37,4 / 34,8 / 16,6	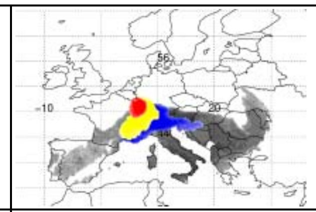	- Sources: South. South-west Germany, Switzerland, Northern Italy, Vosges (France), (Austria). - Background: Southern Europe, Mediterranean Sea. - Model overestimates concentration - unknown loss. Rainy in the south.
2	06-11-15	-21.30 ± 0.42	29.39 ± 3.23	-23.48	23.96	51.75	48.25	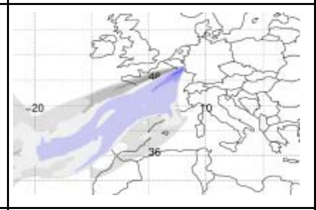	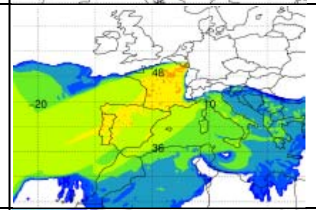	35,6 / 36,1 / 19,8 / 08,5	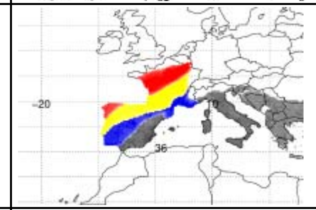	- Sources: West. Luxemburg, Southern Belgium, Central France. - Background: South-west Europe, Mediterranean Sea, Atlantic Ocean. - Light rain in the north
3	10-11-15	-22.89 ± 0.31	12.36 ± 1.36	-23.35	44.45	27.90	72.10	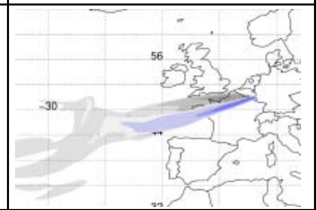	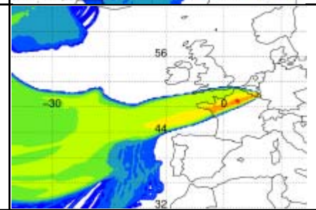	67,5 / 32,5 / 00,0 / 0,00	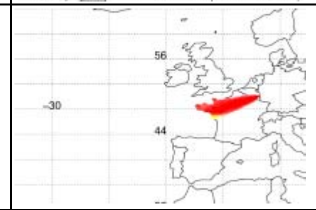	- Sources: West. Luxemburg, Southern Belgium, Southern France. - Background: Atlantic Ocean, northern part. - Model overestimates concentration - unknown loss. - Precipitation in the direction of the retroplume.
4	14-11-15	-22.96 ± 0.37	26.54 ± 2.92	-23.49	28.93	42.86	57.14	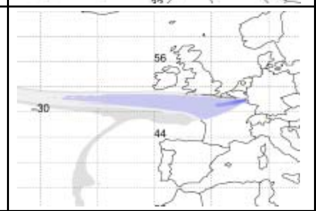	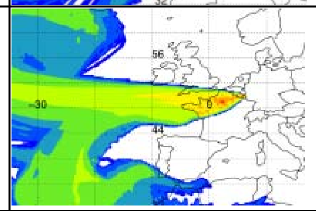	80,8 / 19,2 / 00,0 / 0,00	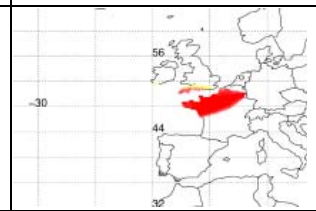	- Sources: West. Luxemburg, Southern Belgium, Southern France. - Background: Atlantic Ocean, northern part. - Light precipitation.
5	22-11-15	-24.64 ± 0.80	35.43 ± 3.90	-23.63	19.78	62.69	37.31	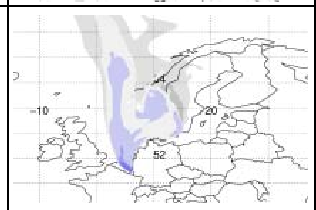	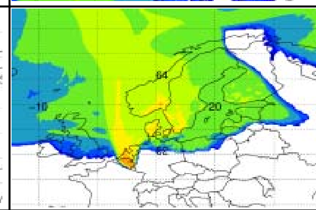	52,6 / 32,1 / 11,4 / 3,99	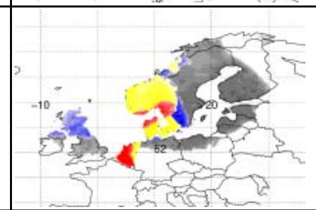	- Sources: North. Benelux, (GB), (Northern Germany), (Scandinavia). - Background: North Sea, Norwegian Sea. - Precipitation.
6	26-11-15	-23.13 ± 0.23	38.51 ± 4.24	-23.68	19.48	63.65	36.35	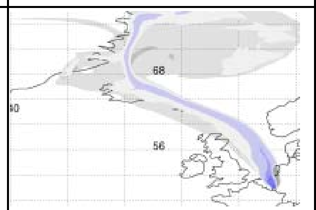	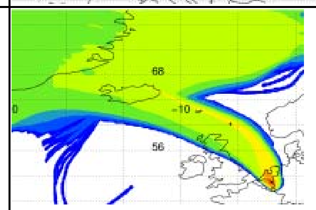	80,6 / 19,4 / 00,0 / 0,00	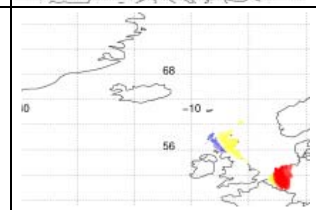	- Sources: North. Benelux, (Northern GB). - Background: Norwegian Sea, incl. Iceland and Greenland. - Light precipitation.
7	08-12-15	-23.17 ± 0.15	70.23 ± 7.73	-23.11	47.03	26.37	73.63	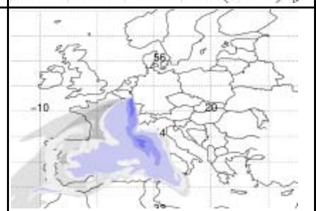	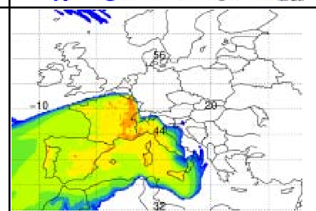	19,9 / 42,6 / 16,4 / 21,0	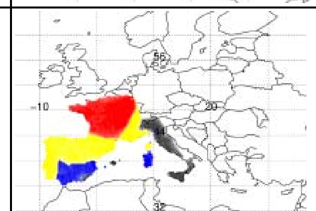	- Sources: West. Luxemburg, France, (Spain), (Italy). - Background: Mediterranean Sea, Atlantic Ocean. - Precipitation.
8	10-02-16	-24.37 ± 0.42	18.18 ± 2.00	-23.53	26.37	47.02	52.98	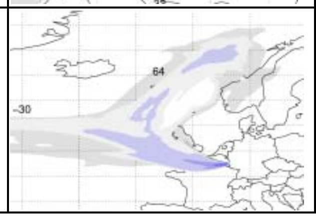	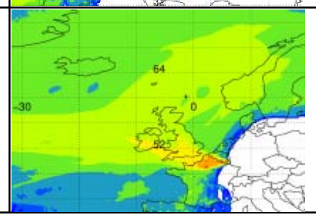	63,5 / 34,0 / 0,17 / 2,37	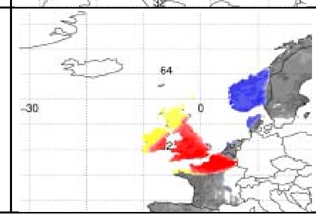	- Sources: West, (North-West). Luxemburg, Northern France, GB, (Scandinavia). - Background: Norwegian Sea, Alantic Ocean (Iceland, Greenland). - Precipitation.

Overview EIFE 2/3

9	14-02-16	-23.65 ± 1.27	78.00 ± 8.58	-23.05	79.93	15.51	84.49	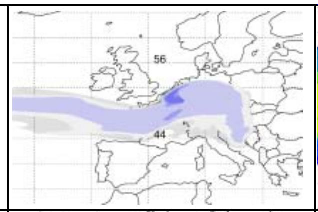	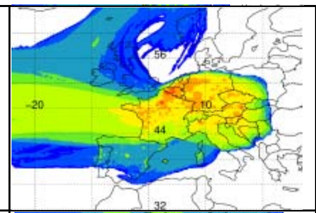	16,2 / 57,0 / 19,8 / 6,96	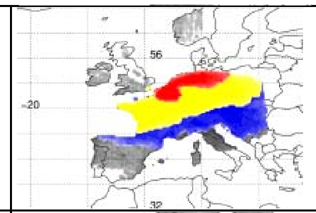	- Sources: Central. Central Europe. - Background: Atlantic Ocean, (Norwegian Sea). - Occasional precipitation.
10	18-02-16	-22.80 ± 0.22	105.35 ± 11.59	-22.88	50.91	24.35	75.65	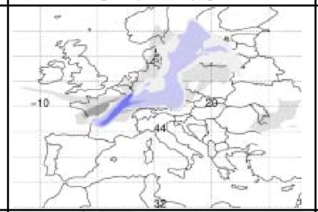	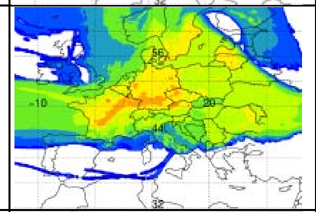	06,4 / 18,0 / 30,3 / 45,4	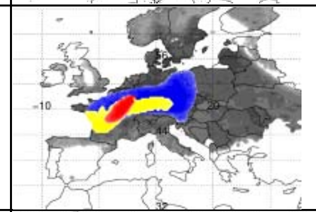	- Sources: Central, (West). Central Europe. - Background: Atlantic Ocean, Baltic Sea, (Norwegian Sea). - Very few precipitation.
11	26-02-16	-23.99 ± 0.42	77.5 ± 8.53	-23.32	36.90	33.60	66.40	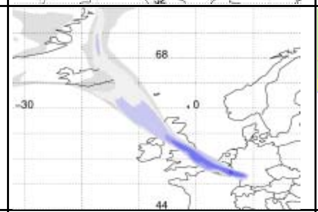	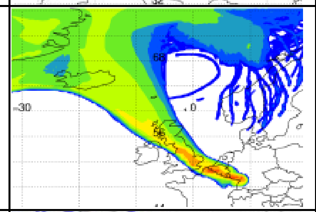	31,4 / 57,9 / 10,3 / 0,44	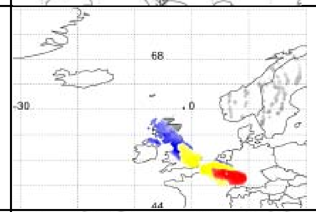	- Sources: North-West. Western Germany, Belgium, Luxemburg, northern France, GB. - Background: Norwegian Sea, (Iceland), (Greenland). - No precipitation in the direction of the retroplume.
12	05-03-16	-25.70 ± 0.42	39.99 ± 4.40	-23.30	39.11	31.70	68.30	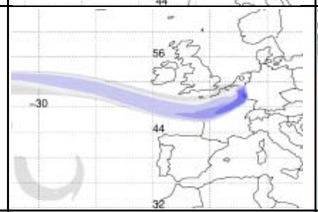	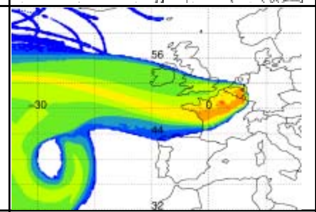	22,1 / 76,7 / 1,20 / 0,00	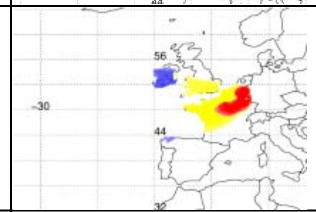	- Sources: West, (North-West). Western Germany, Benelux, GB. - Background: Atlantic Ocean. - Precipitation.
13	09-03-16	-24.06 ± 1.28	58.93 ± 6.48	-23.06	52.10	23.80	76.20	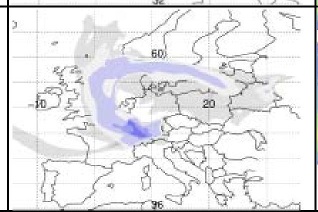	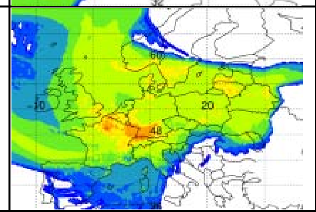	26,6 / 35,9 / 15,1 / 22,4	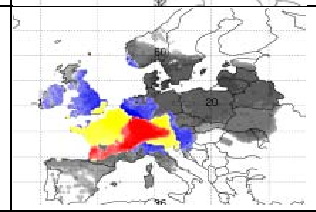	- Sources: Central, (West). Central Europe, mainly Southern Germany, Austria, Luxemburg, north-east France. - Background: Full Europe, Mediterranean Sea, Atlantic Ocean, Norwegian Sea, Baltic Sea. - Light precipitation in the direction of the retroplume.
14	13-03-16	-22.96 ± 0.51	48.97 ± 5.39	-23.22	36.08	34.37	65.63	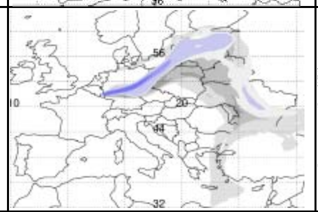	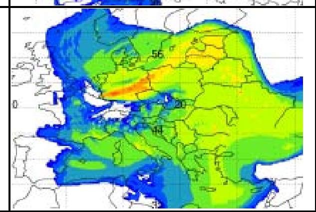	29,7 / 36,8 / 10,6 / 22,8	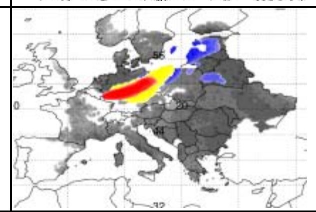	- Sources: Central, (East). Central German, Poland, Baltic States, (Eastern Europe). - Background: Norwegian Sea, Mediterranean Sea, Baltic Sea. - Light precipitation in the direction of the retroplume.
15	17-03-16	-23.06 ± 0.25	88.65 ± 9.75	-23.01	60.03	20.66	79.34	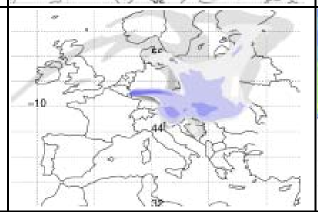	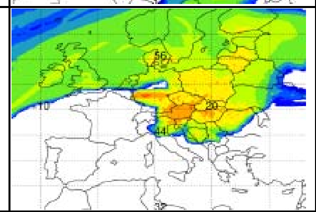	18,4 / 30,8 / 23,0 / 27,8	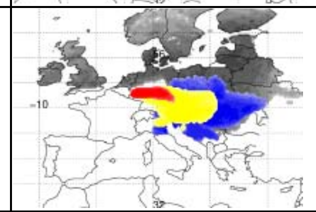	- Sources: East. Central Germany, Switzerland, Czech Republik, Southeast Europe, (northern Europe). - Background: Norwegian Sea. - No precipitation.
16	19-01-17	-23.76 ± 1.24	104.41 ± 11.49	-23.27	38.93	31.85	68.15	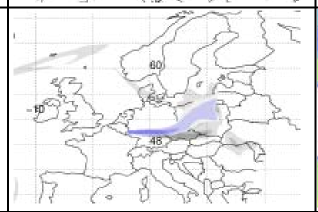	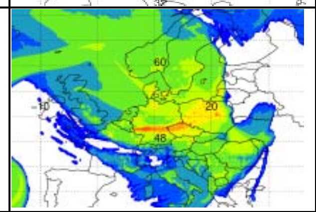	45,1 / 33,6 / 7,96 / 13,4	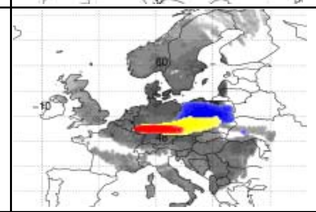	- Sources: East. Central Germany, Czech Republic, Poland. - Background: Baltic Sea, Norwegian Sea. - No precipitation in the direction of the retroplume.
17	27-01-17	-22.54 ± 0.49	103.90 ± 11.43	-22.98	65.05	19.06	80.94	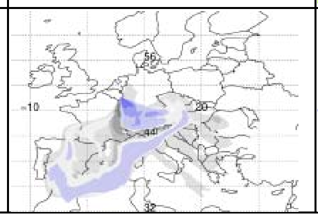	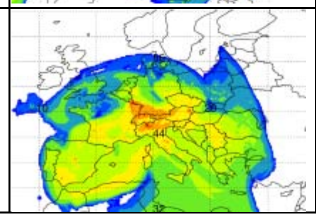	19,8 / 36,1 / 16,8 / 27,4	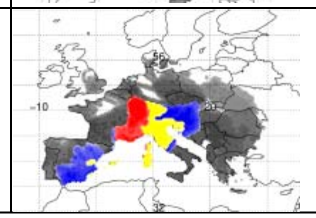	- Sources: South. Southern Germany, Western France, Austria, Switzerland, Northern Italy, (Europe). - Background: Mediterranean Sea, North Sea, Africa. - Model overestimates concentration - unknown loss. - Heavy rain in source regions.

Overview EIFE 3/3

18	12-02-17	-21.82 ± 0.84	156.74 ± 17.24	-22.87	98.36	12.61	87.39	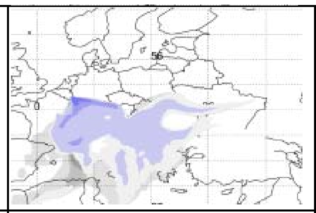	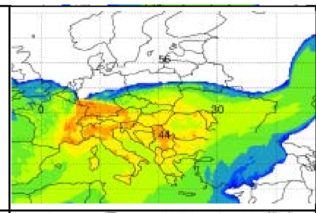	14,2 / 37,5 / 16,8 / 31,5	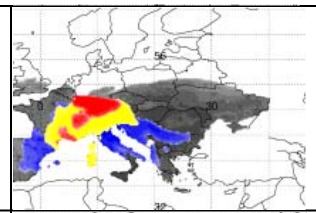	- Sources: South. Southern Germany, Austria, Switzerland, Western France, Northern Italy, (Southeast Europe). - Background: Mediterranean Sea. - Model overestimates concentration - unknown loss. - Light precipitation.
19	20-03-17	-25.78 ± 0.42	19.16 ± 2.11	-23.46	31.37	39.53	60.47	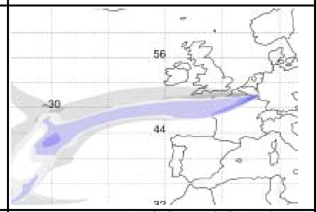	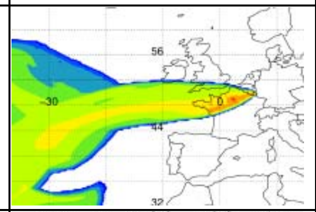	63,0 / 37,0 / 0,00 / 0,00	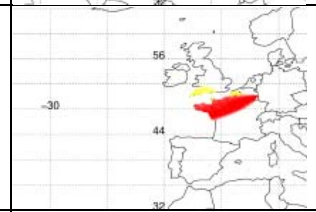	- Sources: West, (North-West). Luxemburg, Southern Belgium, Northern France. - Background: Atlantic Ocean. - Heavy precipitation.
20	24-03-17	-23.66 ± 0.21	72.16 ± 7.94	-22.97	61.40	20.19	79.81	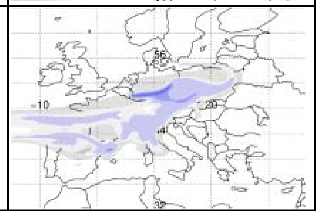	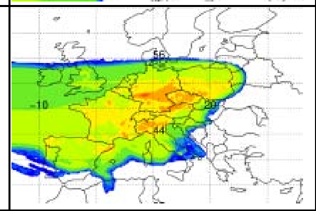	16,3 / 21,1 / 25,6 / 37,0	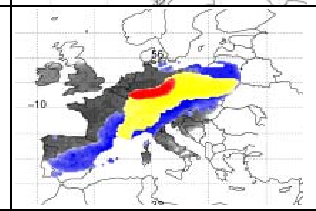	- Sources: East. Central Germany, Czech Republic, Poland, Central Europe. - Background: Atlantic Ocean. - Precipitation in source regions.
21	28-03-17	-22.80 ± 0.42	27.86 ± 3.06	-23.17	51.47	24.09	75.91	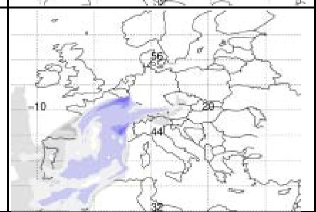	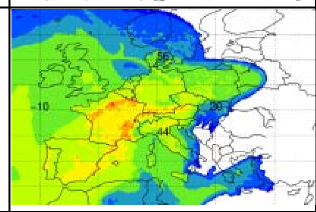	41,9 / 23,8 / 22,3 / 11,9	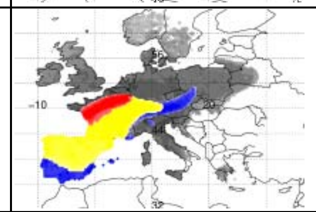	- Sources: South, (West). South-west Germany, Austria, Northern Italy, France, Luxemburg, (Spain). - Background: Mediterranean Sea, North Sea, Atlantic Ocean, Baltic Sea. - Very few precipitation.
22	01-04-17	-24.29 ± 0.34	32.16 ± 3.54	-23.53	20.72	59.85	40.15	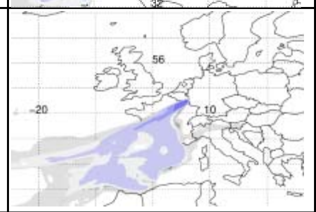	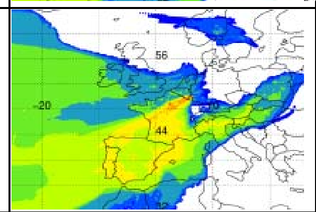	34,5 / 34,5 / 11,1 / 19,9	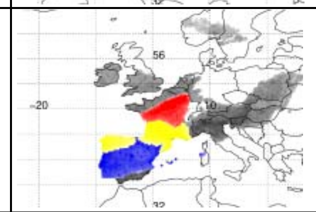	- Sources: West. Luxemburg, Southern Belgium, Central France, (Spain), (GB). - Background: Atlantic Ocean. - Precipitation on sampling day.
23	13-04-17	-23.83 ± 0.26	16.32 ± 1.80	-23.67	19.48	63.65	36.35	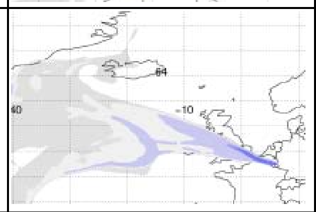	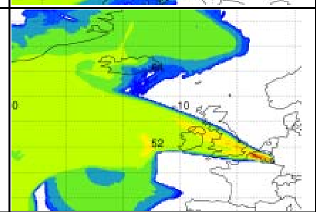	69,2 / 30,7 / 0,09 / 0,00	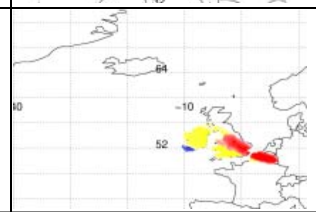	- Sources: North-West. Luxemburg, Belgium, GB. - Background: Northern Atlantic, (Iceland), (Greenland). - Precipitation on sampling day.
24	17-04-17	-23.11 ± 0.45	18.87 ± 2.08	-23.66	19.68	63.00	37.00	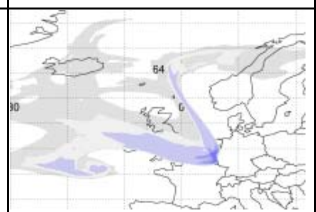	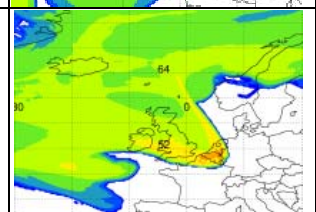	57,8 / 41,6 / 0,33 / 0,24	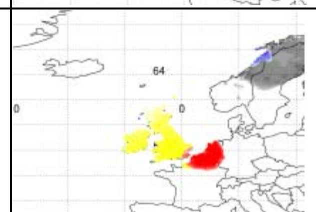	- Sources: North-West. Northern France, Luxemburg, Belgium, Netherlands, Western Germany, (GB). - Background: North Sea, Norwegian Sea, Atlantic Ocean, (Iceland). - Precipitatin on sampling day.
25	21-04-17	-23.55 ± 0.31	30.19 ± 3.32	-23.46	24.98	49.63	50.37	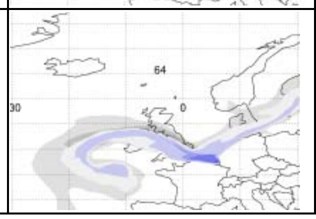	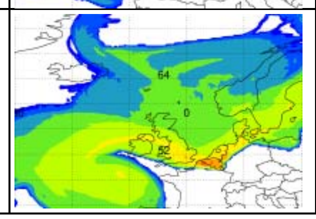	27,5 / 47,5 / 16,9 / 8,01	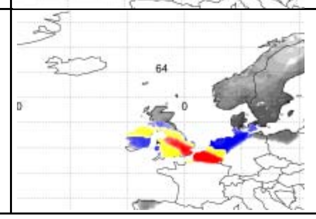	- Sources: North-West. Northern France, Luxemburg, Belgium, Netherlands, Northern Germany, (GB), (Scandinavia). - Background: North Sea, Norwegian Sea, Atlantic Ocean, Baltic Sea. - Very few precipitation in the direction of the retroplume.

Overview STYR 1/3

δ emis (t=0) = -23.2029 ‰
δ backgr = -23.9931 ‰
c backgr = 12.4 ng/m^3

Number	Date	δ exp [‰]	c exp [ng/m^3]	δ mod [‰]	c mod [ng/m^3]	backgr mod [%]	emis mod [%]	Plume (footprint layer, background)	Folded plume (incl. background)	emis mod day1 / 2 / 3 / r [%]	Emission contribution(d1, d2, d3, r)	Info
1	02-11-15	-24.05 ± 0.83	509.48 ± 56.04	-23.09	81.17	15.28	84.72	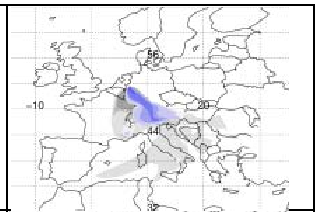	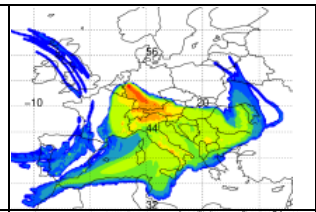	38.0 / 33.3 / 19.0 / 9.70	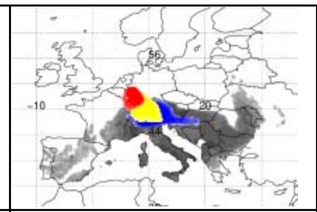	- Sources: South. South-West Germany, Austria, Switzerland, Northern Italy, Slowenia, (South Europe) - Background: South Europe, Mediterranean Sea - Rainy in the south. Model overestimates concentration.
2	06-11-15	-22.56 ± 0.52	58.91 ± 6.48	-23.32	42.43	29.22	70.78	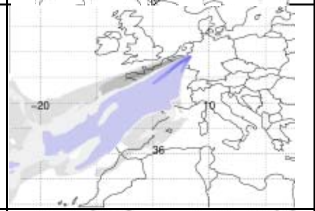	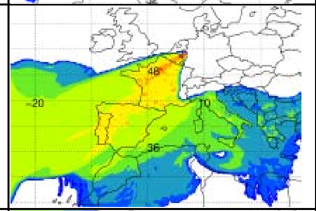	66.7 / 19.3 / 10.2 / 3.84	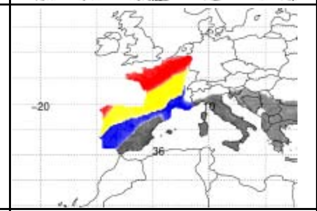	- Sources: West. Limburg, Belgium, Luxemburg, France, Spain, Portugal, (South-West Europe) - Background: Atlantic Ocean, Mediterranean Sea, South-West Europe, (Africa) - Light rain in the north.
3	10-11-15	-25.12 ± 0.42	33.25 ± 3.66	-23.51	28.66	43.27	56.73	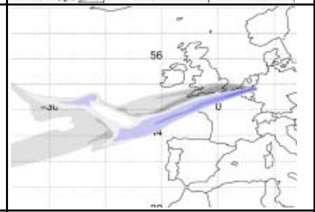	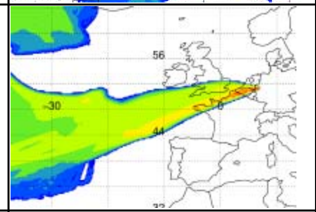	80.6 / 19.4 / 0.00 / 0.00	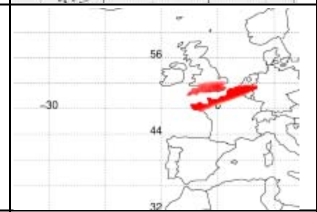	- Sources:West. South Netherlans, Belgium, North of France, (Southern UK). - Background: Atlantic Ocean, (Northern Atlantic Ocean). - Precipitation in the direction of the retroplume.
4	14-11-15	-23.34 ± 1.18	47.61 ± 5.24	-23.56	25.89	47.89	52.11	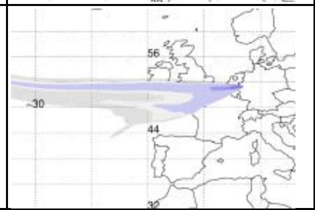	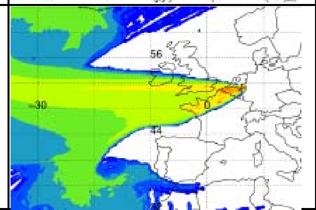	92.1 / 7.89 / 0.00 / 0.00	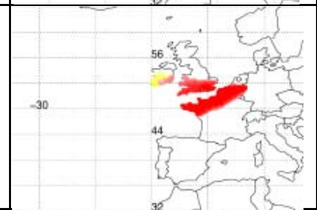	- Sources: West. South Netherlans, Belgium, North of France, (Southern UK). - Background: Atlantic Ocean, (Northern Atlantic Ocean). - Light precipitation.
5	22-11-15	-22.83 ± 0.42	71.70 ± 7.89	-23.63	21.02	59.00	41.00		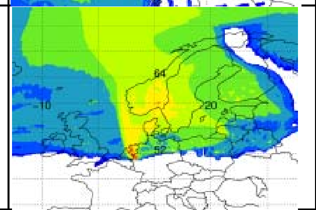	78.5 / 14.7 / 4.76 / 1.99	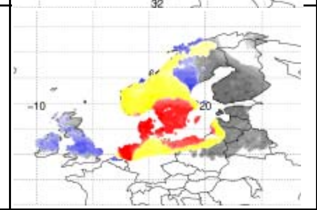	- Sources: North. Netherlands, Scandinavia, (Northern Europe). - Background: Northern Europe including Oceans. - Precipitation.
6	26-11-15	-23.11 ± 0.18	208.13 ± 22.89	-23.60	24.26	51.12	48.88	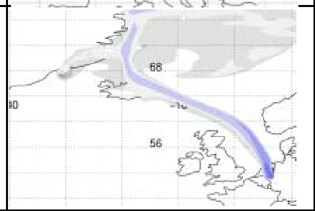	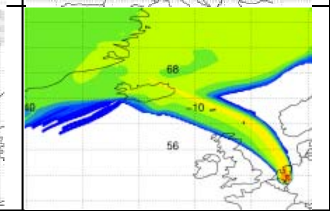	95.4 / 4.64 / 0.00 / 0.00	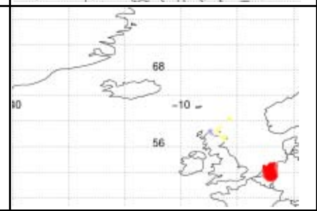	- Sources: North. Southern Belgium, Netherlands, (Northern UK), (Iceland?). - Background: Norwegian Sea including Iceland and Greenland. - Light precipitation. Measurements strongly influenced by local sources.
7	08-12-15	-22.14 ± 0.75	81.91 ± 9.01	-23.15	56.56	21.92	78.08	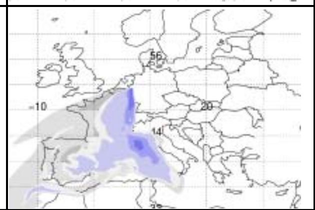	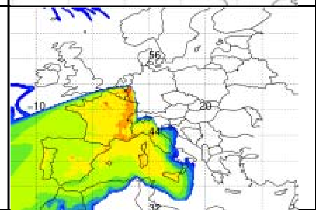	40.1 / 33.5 / 13.7 / 12.7	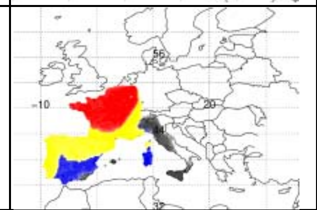	- Sources: West. Western Germany, Limburg, Belgium, France, Northern Italy, Spain, Portugal. - Background: Mediterranean Sea, Southern Atlantic Ocean, (Africa). - Precipitation.
8	10-02-16	-21.79 ± 0.94	52.71 ± 5.80	-23.49	29.84	41.55	58.45	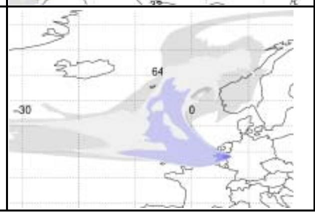	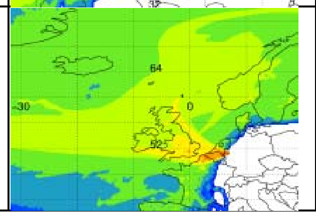	72.6 / 23.8 / 0.37 / 3.26	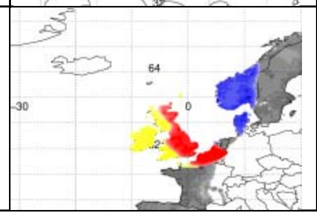	- Sources: West, (North-West). Netherlands, Belgium, Southern France, UK, (France), (Scandinavia). - Background: Northwest Europe, Norwegian Sea, Atlantic Ocean, (Iceland), (Greenland). - Precipitation.

9	14-02-16	-23.73 ± 1.58	207.06 ± 22.78	-23.06	152.61	8.13	91.87	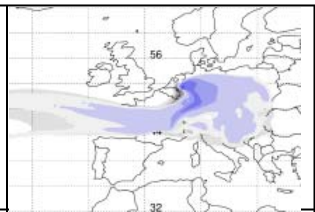	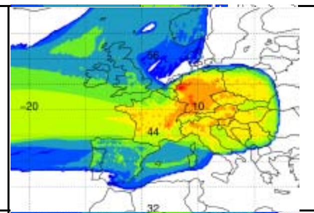	42.2 / 40.6 / 12.1 / 5.05	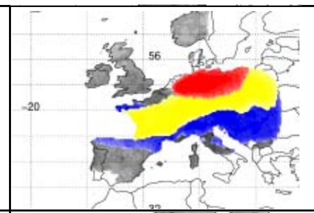	- Sources: Central. Mainly Germany, Poland, Czech Republic, Switzerland, Austria, Northern Italy, France, (Central to Eastern Europe). - Background: Atlantic Ocean, (Norwegian Sea), Mediterranean Sea. - Occasional precipitation. Model overestimates concentration.
10	18-02-16	-22.87 ± 0.32	199.39 ± 21.93	-22.91	75.21	16.49	83.51		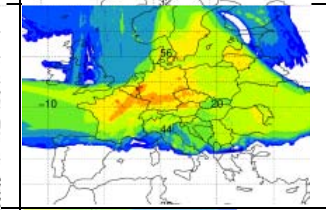	26.7 / 19.6 / 22.3 / 31.4	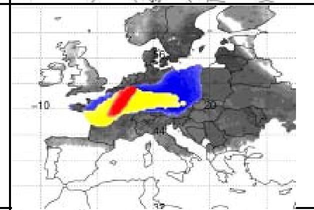	- Sources: Central, (West). Germany, Czech Republic, Switzerland, Central France, (Europe). - Background: Baltic Sea, Atlantic Ocean, (Norwegian Sea), (Mediterranean Sea). - Very few precipitation.
11	26-02-16	-26.26 ± 0.42	189.86 ± 20.88	-23.32	55.14	22.49	77.51	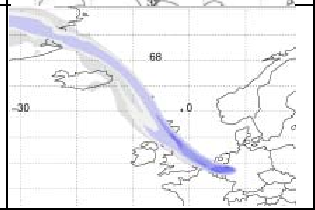	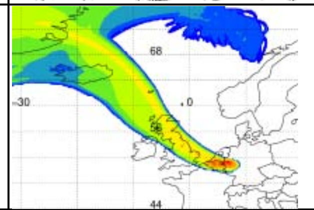	81.7 / 17.0 / 1.29 / 0.00	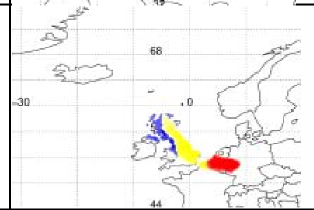	- Sources: North-West. Southern Netherlands, Belgium, UK. - Background: Direction Greenland and Iceland. - No precipitation in the direction of the retroplume.
12	05-03-16	-22.80 ± 0.16	282.26 31.05	-23.18	108.46	11.43	88.57	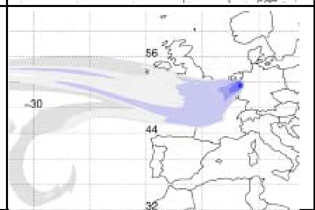	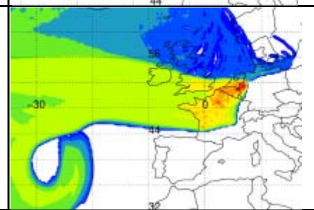	59.7 / 38.6 / 1.74 / 0.00	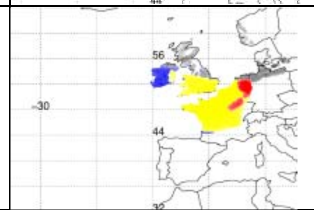	- Sources: West, (North-West). Netherlands, Belgium, Northern France, (Southern UK). - Background: Atlantic Ocean. - Precipitation.
13	09-03-16	-24.02 ± 0.42	95.21 ± 10.47	-23.01	64.39	19.26	80.74	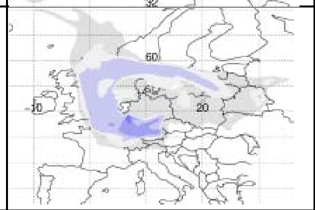	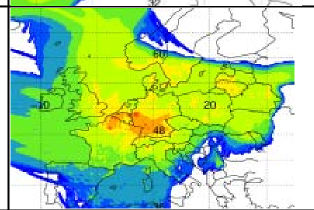	34.6 / 28.3 / 11.9 / 25.9	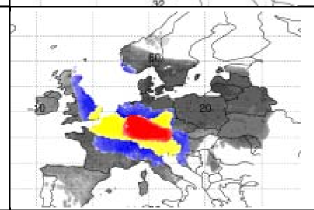	- Sources: Central, (West). Central Germany, Belgium, South-East France, (Europe). - Background: Norwegian Sea, (Atlantic Ocean), (Mediterranean Sea). - Light precipitation in the direction of the retroplume.
14	13-03-16	-24.48 ± 0.42	85.26 ± 9.38	-23.26	44.16	28.08	71.92	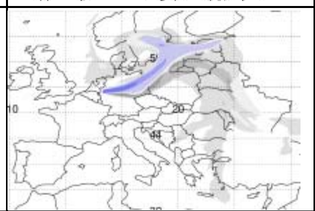	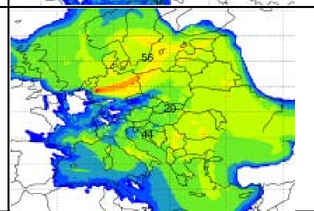	63.2 / 20.3 / 2.14 / 14.4	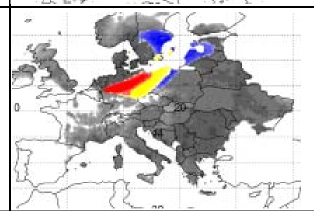	- Sources: Central, (East). Central Germany, Poland, (North-West Europe). - Background: Baltic Sea, Norwegian Sea, (Mediterranean Sea). - Light precipitation in the direction of the retroplume.
15	17-03-16	-23.60 ± 1.45	217.82 ± 23.96	-23.17	67.41	18.40	81.60		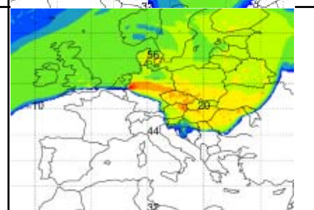	55.3 / 24.2 / 8.82 / 11.7	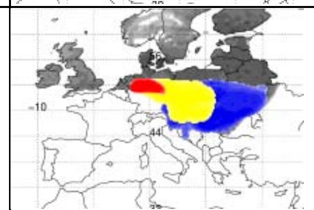	- Sources: East. Central Germany, Switzerland, Czech Republic, Poland, Eastern Europe, (Scandinavia). - Background: Baltic Sea, Norwegian Sea, (Atlantic Ocean). - No precipitation. Measurements strongly influenced by local sources.
16	19-01-17	-22.15 ± 0.40	434.85 ± 47.83	-23.33	51.36	24.14	75.86	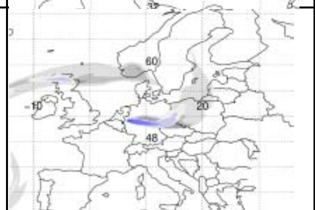	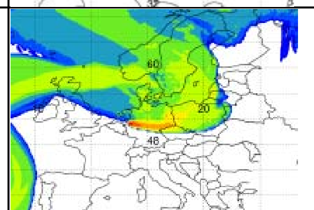	76.9 / 17.9 / 3.27 / 1.95	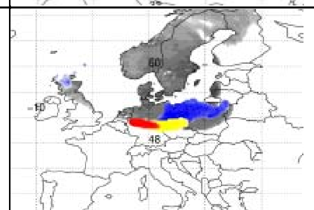	- Sources: East. Central Germany, Poland, Southern Czech Republic, Baltic States, Scandinavia. - Background: Baltic Sea, Norwegian Sea. - No precipitation in the direction of the retroplume. Measurements strongly influenced by local sources.
17	27-01-17	-23.10 ± 0.20	281.86 ± 31.00	-23.00	91.16	13.60	86.40	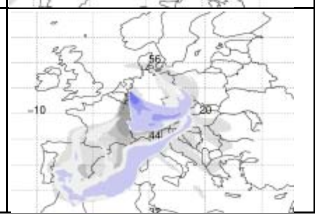	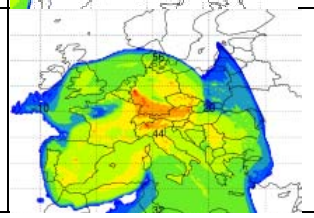	32.2 / 31.8 / 16.4 / 19.5	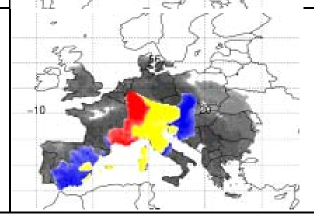	- Sources: South. Southern Germany, Czech Republic, Switzerland, Northern Italy, Austria, (Whole Europe). - Background: (North Sea), (Mediterranean Sea). - Heavy rain in source regions. Model overestimates concentration.

Overview STYR 3/3

18	12-02-17	-22.31 ± 0.61	248.32 ± 27.32	-22.88	112.18	11.05	88.95	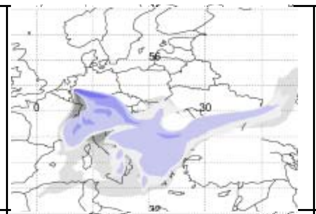	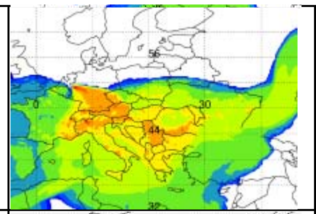	19.2 / 30.4 / 19.9 / 30.5	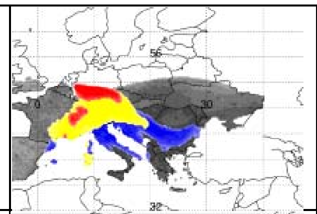	- Sources: South. Central Germany, Czech Republic, Switzerland, Slowenia, Croatia, Hungary, (South-East Europe). - Background: Mediterranean Sea, (Africa), (Asia). - Light precipitation.
19	20-03-17	-24.47 ± 0.42	158.45 ± 17.43	-23.46	33.47	37.05	62.95	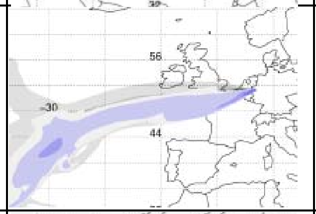	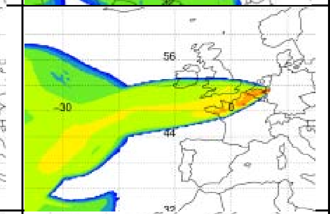	83.8 / 16.2 / 0.00 / 0.00	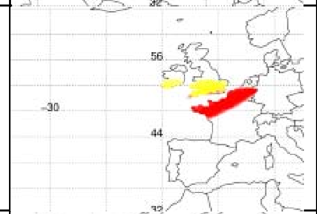	- Sources: West, (North-West). Southern Netherlands, Belgium, Southern UK, Northern France. - Background: Atlantic Ocean. - Heavy precipitation. Measurements strongly influenced by local sources.
20	24-03-17	-23.06 ± 0.40	77.99 ± 8.58	-23.13	57.77	21.46	78.54	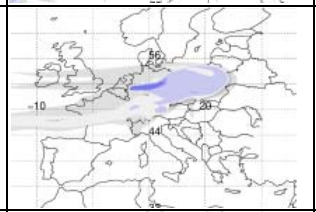	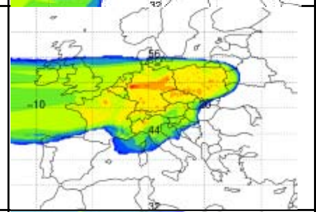	41.7 / 20.8 / 13.6 / 23.8	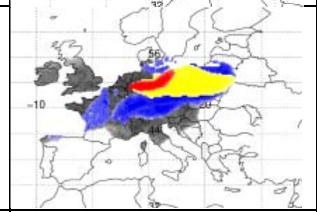	- Sources: East. Central Germany, Poland, Czech Republic, Central Europe. - Background: Atlantic Ocean, (Norwegian Sea), (Mediterranean Sea). - Precipitation in source regions.
21	28-03-17	-23.30 ± 0.36	48.67 ± 5.35	-23.06	76.51	16.21	83.79	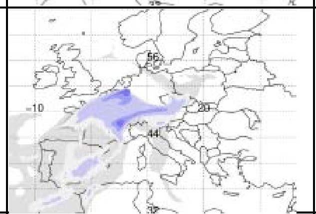	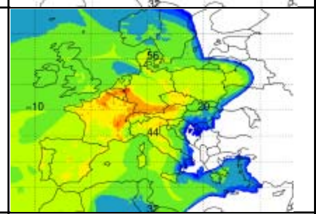	33.6 / 27.3 / 22.9 / 16.2	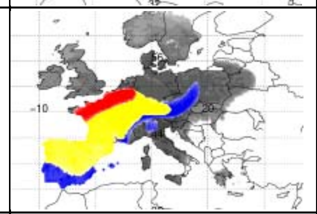	- Sources: South, (West). Southwest Germany, Limburg, Belgium, Northern France, Austria, Switzerland, South Europe, (Central Europe). - Background: All Oceans around Europe, (Africa). - Very few precipitation.
22	01-04-17	-23.36 ± 0.30	69.28 ± 7.62	-23.35	36.94	33.57	66.43	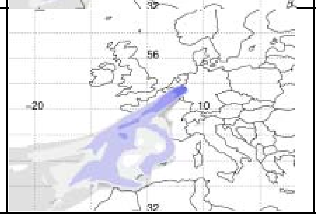	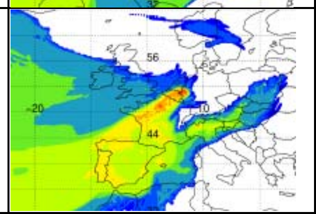	50.6 / 41.0 / 4.06 / 4.30	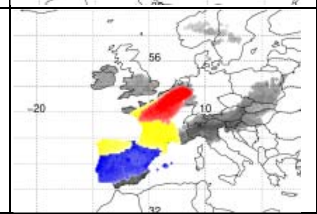	- Sources: West. Limburg, Belgium, France, (Spain), (Portugal), (Northern Italy). - Background: Atlantic Ocean, (Mediterranean Sea). - Precipitation on sampling day.
23	13-04-17	-24.73 ± 0.81	25.41 ± 2.80	-23.77	16.99	72.98	27.02	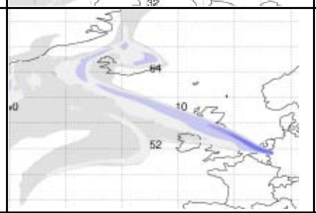	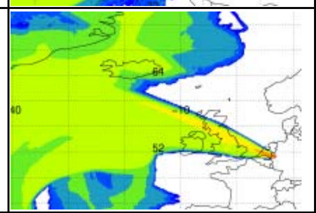	89.1 / 10.9 / 0.02 / 0.00	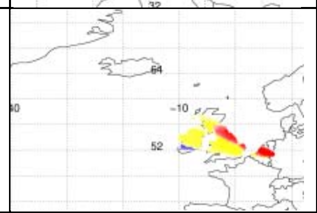	- Sources: North-West. Netherlands, Northern Belgium, UK. - Background: Northern Atlantic Ocean, (Iceland), (Greenland). - Precipitation on sampling day.
24	17-04-17	-22.47 ± 0.27	37.79 ± 4.16	-23.64	21.74	57.03	42.97	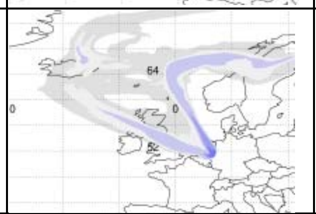	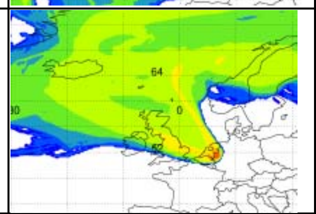	82.6 / 16.9 / 0.11 / 0.37	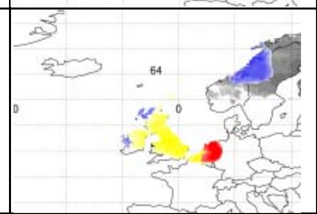	- Sources: North-West. Netherlands, Northern Belgium, Northern UK, (Northern Scandinavia). - Background: Norwegian Sea. - Precipitation on sampling day.
25	21-04-17	-24.08 ± 0.16	80.05 ± 8.81	-23.60	21.23	58.40	41.60	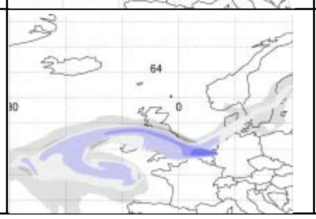	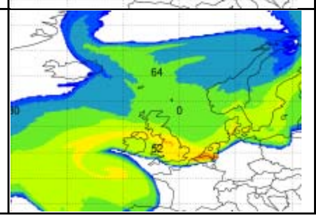	56.7 / 28.8 / 6.78 / 7.69	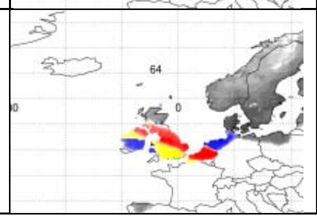	- Sources: North-West. Netherlands, Northern Belgium, UK, Northern France, Northern Germany, (Scandinavia). Background: Atlantic Ocean, (Norwegian Sea), (Baltiv Sea). - Very few precipitation in the direction of the retroplume.